MOLECULAR AND CELLULAR BIOLOGY, May 2009, p. 2469–2480 Vol. 29, No. 9
0270-7306/09/$08.00+0 doi:10.1128/MCB.01304-08

A Role for a CXCR2/Phosphatidylinositol 3-Kinase γ Signaling Axis in Acute and Chronic Vascular Permeability▽†

Julie Gavard,[1,4,5]* Xu Hou,[2] Yi Qu,[2] Andrius Masedunskas,[1,3] Daniel Martin,[1] Roberto Weigert,[1,3] Xuri Li,[2] and J. Silvio Gutkind[1]*

Oral and Pharyngeal Cancer Branch, National Institute of Dental and Craniofacial Research, National Institutes of Health, 30 Convent Drive, Rm. 211, Bethesda, Maryland 20892[1]; Unit of Vascular Retinal Neurobiology Research, Porter Neuroscience Research Center, National Eye Institute, National Institutes of Health, 35 Lincoln Drive, Rm. 2A-108, MSC 3731, Bethesda, Maryland 20892[2]; Intracellular Membrane Trafficking Unit, Oral and Pharyngeal Cancer Branch, National Institute of Dental and Craniofacial Research, National Institutes of Health, 30 Convent Drive, Rm. 303A, Bethesda, Maryland 20892[3]; Institut Cochin, Universite Paris Descartes, CNRS (UMR 8104), Paris, France[4]; and INSERM, U567, Paris, France[5]

Received 16 August 2008/Returned for modification 20 October 2008/Accepted 2 February 2009

Most proangiogenic polypeptide growth factors and chemokines enhance vascular permeability, including vascular endothelial growth factor (VEGF), the main target for anti-angiogenic-based therapies, and interleukin-8 (IL-8), a potent proinflammatory mediator. Here, we show that in endothelial cells IL-8 initiates a signaling route that converges with that deployed by VEGF at the level of the small GTPase Rac1 and that both act through the p21-activated kinase to promote the phosphorylation and internalization of VE-cadherin. However, whereas VEGF activates Rac1 through Src-related kinases, IL-8 specifically signals to Rac1 through its cognate G protein-linked receptor, CXCR2, and the stimulation of the phosphatidylinositol 3-kinase γ (PI3Kγ) catalytic isoform, thereby providing a specific molecular targeted intervention in vascular permeability. These results prompted us to investigate the potential role of IL-8 signaling in a mouse model for retinal vascular hyperpermeability. Importantly, we observed that IL-8 is upregulated upon laser-induced retinal damage, which recapitulates enhanced vascularization, leakage, and inflammatory responses. Moreover, blockade of CXCR2 and PI3Kγ was able to limit neovascularization and choroidal edema, as well as macrophage infiltration, therefore contributing to reduce retinal damage. These findings indicate that the CXCR2 and PI3Kγ signaling pathway may represent a suitable target for the development of novel therapeutic strategies for human diseases characterized by vascular leakage.

During embryonic development, blood vessels arise from endothelial precursors which share their origin with hematopoietic precursors (8). These progenitors assemble into a primitive vascular network of small capillaries, through a process called vasculogenesis, and this vascular plexus progressively expands and remodels into a highly organized pattern by the growth of blood vessels from preexisting ones, a process referred to as angiogenesis (8). During adulthood, endothelial cells that form the vascular wall retain their plasticity and can be engaged in neovascularization in response to physiological stimuli, such as hypoxia, wound healing, and tissue repair. In addition, numerous human diseases and pathological conditions are characterized by an excessive, uncontrolled, and aberrant angiogenesis (35). This physiological process is often co-opted by tumor cells to build a new vascular network dedicated to supply oxygen and nutrients to the cancerous cells, thereby enabling them to proliferate and metastasize (16).

Aberrant angiogenesis occurs in numerous pathological conditions, such as in acute and chronic inflammation, thrombotic reactions, edema, tumor-induced angiogenesis, and metastasis (35). For example, this process is central to the progression of many ocular diseases, where blood vessels show a disorganized and anarchic pattern and are frequently leaky (17). Indeed, the breakdown of the endothelial barrier, characterized by an uncontrolled increase in vascular permeability, contributes to edema formation and inflammation in many pathological conditions (49). The enhanced endothelial permeability can be mediated through transcellular and paracellular mechanisms. Of note, the transcellular passage of plasma molecules and cells requires either cell fenestration or a complex system of vesiculo-vacuolar organelle transport, while the paracellular passage is achieved by the coordinated opening and closure of endothelial cell-cell junctions (49). This barrier function of the endothelium requires the adhesive activity of VE-cadherin and claudin-5, which are key components of the adherens and tight endothelial junctions, respectively (9). The formation, maintenance, and remodeling of the intercellular contacts involve a functional interaction between these two adhesive structures. It has been demonstrated recently that the expression of claudin-5 is directly controlled through VE-cadherin adhesion, therefore placing VE-cadherin upstream in the control of the endothelial barrier integrity (45). Moreover, vascular endothe-

* Corresponding author. Mailing address for J. Silvio Gutkind: Oral and Pharyngeal Cancer Branch, National Institute of Dental and Craniofacial Research, National Institutes of Health, 30 Convent Drive, Rm. 211, Bethesda, MD 20892. Phone: (301) 496-6259. Fax: (301) 402-0821. E-mail: sg39v@nih.gov. Mailing address for Julie Gavard: Institut Cochin, CNRS (UMR8104), INSERM, U567, Université Paris Descartes, 22 rue Mechain, 75014 Paris, France. Phone: 33-140-516-24. Fax: 33-140-516-30. E-mail: julie.gavard@inserm.fr.

† Supplemental material for this article may be found at http://mcb.asm.org/.

▽ Published ahead of print on 2 March 2009.

lial growth factor A (VEGF-A) increases vascular permeability through a signaling pathway involving the sequential activation of Src, Vav2, Rac, and p21-activated kinase (PAK), which culminates in the phosphorylation of VE-cadherin, thus provoking endothelial cell-cell junction destabilization (18–20, 32, 43, 46, 48).

In the past few years, progress has been made in the pharmacological inhibition of proangiogenic mechanisms, with a focal effort on VEGF-A, as this cytokine plays a key role in the promotion of neovascularization and vascular leakage (16, 21, 31, 40). However, anti-VEGF therapies are not suitable for all patients, as they may affect the function of the normal vasculature, and in the case of ocular diseases, they may require repeated patient visits and demanding clinical procedures, with some transient yet serious adverse events (15, 21, 52). Thus, understanding the mechanisms that contribute to pathological vascular leakage may help in identifying novel therapeutic targets. Of interest, interleukin-8 (IL-8; CXCL-8) plays multiple functions in angiogenesis by stimulating endothelial cell growth, permeability, and migration and by serving as a potent chemoattractant factor for lymphocytes, macrophages, and neutrophils, thus providing an inflammatory vascular bed (10, 24, 26, 34, 37, 44, 53). While the contribution of IL-8 release to inflammatory processes has been extensively documented (6), its participation in pathologies that involved aberrant angiogenesis and vascular leakage has been poorly explored.

MATERIALS AND METHODS

Cell culture and transfection. Immortalized human vascular endothelial cells were described previously (13). Simian virus 40 (SV40) immortalized mouse endothelial cells (SVEC) and human embryonic kidney cells (HEK-293T) were obtained from the ATCC (Manassas, VA, and Molsheim, France, respectively). DNA transfections of endothelial cells and HEK-293T cells were performed using Amaxa's electroporation system (Amaxa Biosystems, Gaithersburg, MD) and the TurboFECT reagent (Fermentas, Saint-Remy-Les-Chevreuse, France), respectively. Small interfering RNA (siRNA) transfections of the nonsilencing control (Dharmacon, Chicago, IL) and mouse Rac silencing (Invitrogen, Carlsbad, CA) were done with the Hiperfect reagent (Qiagen, Valencia, CA).

Animals. All animal studies were carried out according to NIH-approved protocols, in compliance with the *Guide for the Care and Use of Laboratory Animals* (30a). Ten-week-old female mice (C57BLw), female athymic (*nu*/*nu*) nude mice, and male Sprague-Dawley rats (Harlan Sprague-Dawley, Frederick, MD) were used.

Reagents and antibodies. Recombinant human VEGF and IL-8 were purchased from PeproTech (Rocky Hill, NJ). Wortmannin, SU^{1498} (VEGF receptor 2 [VEGFR2] inhibitor), SU^{6656} (Src family kinase inhibitor), SB^{225002} (CXCR2 inhibitor), and AS^{605240} (phosphatidylinositol 3-kinase γ [PI3Kγ] inhibitor) were from Calbiochem (San Diego, CA), and LY^{294002} was from Ozyme (Saint-Quentin-en-Yvelines, France). The following antibodies were used: anti-Rac (BD Biosciences, San Jose, CA), anti-phospho-extracellular signal-regulated kinase 1/2 (anti-phospho-ERK1/2), phospho PAK1/2, PAK1, phospho S473 AKT, AKT, and PI3Kγ from Cell Signaling, Boston, MA; anti-phospho-Y1054 VEGFR2 from Biosource QCB, Camarillo, CA; VEGFR2, VEGF-A, ERK1/2, RhoA/B/C, and VE-cadherin from Santa Cruz Biotech, Santa Cruz, CA; anti-KC from BioVision, Mountain View, CA; anti-F4/80 from eBiosciences, San Diego, CA; anti-AU5 tag from Clinisciences, Montrouge, France; CXCR2 from Abcam, Cambridge, MA; and anti-phospho-S665 VE-cadherin (19). Secondary antibodies were from Jackson ImmunoResearch (West Grove, PA) and Southern Biotechnology (Birmingham, AL).

DNA constructs. pCEFL-GFP-PAK inhibitory domain (PID), pCEFL-human VE-cadherin wild type (WT), S665V and S665D, pCEFL-AU5 Rac WT, QL, and N17 were previously described (19). Human CXCR2 (#NM_001557) was cloned in frame into the pCEFL-AU5 plasmid. pLKO.1 containing predesigned short hairpin RNAs (shRNAs) against human PI3Kα or -γ subunits (TRCN0000000390603, shα#1; TRCN000000390607, shα#2; TRCN00000033279, shγ #1; and TRCN00000033282, shγ #2) was obtained from Open Biosystems, Huntsville, AL. The efficiency and specificity of each shRNA were evaluated by quantitative reverse transcription-PCR (RT-PCR). pGIPZ lentiviral predesigned human CXCR2 shRNAmir-GFP was purchased from Open Biosystems (Huntsville, AL), and vesicular stomatitis virus-pseudotyped lentiviruses were produced using standard protocols (19). One week later, infected cells were selected with Puromycin (1.5 μg/ml) for 5 days and further selected by fluorescence-activated cell sorting for green fluorescent protein (GFP) expression.

Miles assays and in vitro permeability assays. In vivo permeability assays were conducted as described previously (20). Briefly, sterile Evans blue dye (EB; Sigma) was injected intravenously (150 μl, 1% in 0.9% NaCl) through the tail vein. The saline control (phosphate-buffered saline [PBS]), VEGF (50 ng in 250 μl), and IL-8 (50 ng in 250 μl), alone or in combination with SB^{225002} (50 μM) or AS^{605042} (2 μM), were injected subdermally. The injection zone was marked for further analysis. Mice were kept for 1 h, before sacrificing. Skin samples were dissected, photographed, and either placed in formamide at 56°C for 36 h to extract EB or fixed in ethanol for further frozen sections. Samples fast frozen with dry ice were also saved for Western blot analysis. Noninjected skin samples were used to normalize quantification of EB extravasation, as read by spectrophotometry at the optical density at 620 nm.

In vitro permeability assays were conducted as described previously (19). Briefly, endothelial cells were grown as a mature monolayer on collagen-coated 3-μm-pore-size inserts (PTFE; Corning Costar, Acton, MA). Cells were starved overnight, treated as required, and incubated with fluorescein isothiocyanate (FITC)-conjugated 60-kDa dextran (1 mg/ml; Molecular Probes, Invitrogen). Each sample from the bottom chamber was read in triplicate on the Victor 3V1420 multicounter (Perkin-Elmer, Wellesley, PA). Results are shown as the mean of three independent experiments ± standard error, as calculated by the Prism 4.2 software (GraphPad).

VE-cadherin internalization assay and immunofluorescence. The protocol was described previously (20). Briefly, cells were incubated in Dulbecco's modified Eagle's medium with anti-VE-cadherin (BV6 clone, 1 μg/ml; Research Diagnostics, Inc., Flanders, NJ) at 4°C for 1 h. The antibody uptake was induced for 30 min at 37°C in serum-free medium or in the presence of VEGF and IL-8. Cells were either fixed or subjected to a mild acid wash (PBS–25 mM glycine [pH 2.0] for 15 min) in order to remove plasma membrane-bound antibodies. Immunofluorescence staining was done as described in reference 19. Cryostat sections were obtained from fixed frozen skin samples and treated as described in reference 20. Confocal acquisitions were performed on TCS/SP2 Leica microscope (NIDCR Confocal Facility, NIH, Bethesda, MD; and Institut Cochin Confocal Facility, Paris, France).

Quantitative RT-PCR analysis. Total RNA was isolated with the RNeasy isolation kit (Qiagen). Three micrograms of total RNA was used for each RT reaction using the Superscript II reagent (Invitrogen). Quantitative PCR using the iCycler iQ real-time PCR detection system and iQ SYBR green supermix (Bio-Rad, Hercules, CA) was performed, using primers for PI3Kα (forward, 5′-ATGCCTCCACGACCATCATCAGG-3′; reverse 5′-AAACATTCTACTAGGATTCTTGG-3′), PI3Kγ (forward, 5′-ATGGAGCTGGAGAACTATAAAC-3′; reverse, 3′-GCGGCTTCATCCTCCGGCGCCTT-5′), and 18S rRNA (forward, 5′-CGCCGCTAGAGGTGAAATTC-3′; reverse, 5′-TTGGCAAATGCTTTCGCTC-3′) as an endogenous control for normalization. The comparative threshold cycle ($\Delta\Delta C_T$) analysis method (Genex software; Bio-Rad) was used to assess the relative changes in gene expression. The experiments were repeated in triplicate, and the mean changes ± standard error of the mean are reported.

GST pull-down and Western blot. Rac and Rho activation was monitored by glutathione *S*-transferase (GST) pull-downs, using the GST-PAK-CRIB (Cdc42/Rac interacting binding domain) and GST-Rhotekin recombinant proteins, respectively, bound to glutathione slurry resin (Amersham Biosciences, General Electrics, Piscataway, NJ) as described in reference 30. Cells were lysed in magnesium buffer containing 10 mM Tris (pH 7.5), 100 mM NaCl, 1% Triton X-100, 0.5 mM EDTA, 40 mM β-glycerophosphate, 10 mM $MgCl_2$, 1 mM Na_3VO_4, 10 μg/ml aprotinin, 10 μg/ml leupeptin, and 1 mM phenylmethylsulfonyl fluoride. For Western blot analysis, equal amounts of protein were separated onto 4 to 20% polyacrylamide sodium dodecyl sulfate (SDS)-Tris-glycine gels (Invitrogen) and transferred onto polyvinylidene difluoride membranes (Millipore, Billerica, MA). Horseradish peroxidase activity was revealed by chemiluminescence reaction (ECL kit; Pierce, Rockford, IL). Alternatively, membranes were scanned using the Odyssey infrared imaging system (Li-Cor BioSciences, EuroSep, Cergy-Pontoise, France) and dylight680 fluorescent dye-conjugated secondary antibodies (Thermo Fischer Scientific, Villebon, France).

Laser-induced retinal damage. Ten-week-old female C57BLw mice (Harlan) were anesthetized, and their pupils were dilated (ASP#06-553; NIH-approved animal protocol). Mice were positioned on a rack connected to a slit lamp

delivery system. Four photocoagulation spots were made (75-μm spot size, 75 ms, and 90 mW of power) with the Oculight infrared laser system (810 nm; IRIDEX Corporation) in the area surrounding the optic nerve in each eye. The sites were visualized through a handheld contact lens and a viscous surface lubricant. Only laser-induced burns with a bubble formation were included in the study. The mice were given lubricant ophthalmic ointment after laser treatment. For inhibitor treatment, 0.5 μl of SB^{225002} and AS^{605402} chemicals in 0.01% dimethyl sulfoxide solution per eye was injected into the vitreous just after the laser treatment. A second injection was given 3 days later. The same volume of the vehicle was used for the control group. One or 2 weeks after laser treatment, eyes were removed and fixed, and their retinas were dissected. Choroids were isolated and stained with isolectin B4 conjugated with Alexa Fluor 568 according to the manufacturer's protocol (Invitrogen). After staining, the eyecups were flat-mounted in Aquamount with the sclera facing down and the total neovascular area was measured (AxioVision software; Carl Zeiss, Inc.); the mean value per burn is presented for each eye. Alternatively, eyecups were fixed overnight in PBS buffered 4% paraformaldehyde, transferred to 95% ethanol, and embedded in paraffin. Five-micrometer sections were cut and stained with hematoxylin and eosin (HistoServ, Inc., Gaithersburg, MD).

Two-photon intravital microscopy. Rats were anesthetized and placed on an adjustable stage on the side of an Olympus IX81 microscope. FITC-conjugated 500-kDa dextran (4 mg/kg of body weight in 300 μl; Invitrogen) was injected into the tail vein. IL-8 (50 ng/10 μl), alone or with compounds SB^{225002} and AS^{605240}, was injected subcutaneously into the ears. Blood vessels located 0.2 to 0.5 mm from the injection site were immediately imaged in time-lapse mode for 1 h. FITC was excited with a Chameleon Ultra II infrared beam (800 nm; Coherent, Inc., Palo Alto, CA), attenuated by a 1.0-neutral-density filter and directed through a beam expander into an Olympus Fluoview 1,000-scanning-unit (570-nm dichroic mirror and 500- to 60-nm barrier filter; Chroma Technology). Time-lapse acquisitions were performed at 1 frame/s, and the images were processed using Metamorph (Molecular Devices, CA).

Statistical analysis. Graphs are shown as mean values ± standard errors of the mean from at least three independent experiments, and confocal pictures and Western blot scans are representative of at least three independent experiments. Statistical analysis was performed with Prism software. Analysis of variance (ANOVA) was performed with GraphPad, and *t* tests were performed for the choroidal neovascularization assays ($P < 0.001$, $P < 0.01$, or $P < 0.05$).

RESULTS

VE-cadherin internalization is required for IL-8-induced endothelial monolayer permeability. To investigate the ability of the IL-8 chemokine to affect the endothelial barrier plasticity, we first tested the effect of IL-8 stimulation on endothelial cell-cell junction remodeling in human vascular endothelial cells cultured as a monolayer. Interestingly, we recently found that VEGF, a proangiogenic and propermeability factor, triggers VE-cadherin serine phosphorylation and internalization (19). In line with these findings, we observed that IL-8 induces morphological changes in the architecture of VE-cadherin-containing junctions, concomitant with an increased endocytosis of VE-cadherin (Fig. 1A). The extent of IL-8-induced VE-cadherin antibody uptake was comparable to that provoked by VEGF stimulation (Fig. 1B). To further examine the contribution of VE-cadherin phosphorylation on position 665 to junctional remodeling in response to IL-8, we engineered mouse endothelial cells expressing WT human VE-cadherin or its nonphosphorylatable S665V and phosphomimetic S665D mutants (19). IL-8 normally induced the internalization of human VE-cadherin when expressed in mouse endothelial cells, while the human VE-cadherin S665V mutant failed to do so (Fig. 1C). In contrast, the human VE-cadherin S665D mutant was constitutively internalized even in the absence of IL-8, thereby causing an increased basal permeability (Fig. 1D). Importantly, the noninternalizable VE-cadherin S665V mutant strongly reduced IL-8-induced endothelial permeability. Thus, the IL-8 intracellular signaling pathway appears to converge with that deployed by VEGF on the phosphorylation-dependent endocytosis of VE-cadherin, which may in turn cause the destabilization of interendothelial junctions and enhanced endothelial permeability.

IL-8 increases endothelial monolayer permeability through a CXCR2/Rac/PAK signaling axis. We next tested the intracellular signaling events elicited in human endothelial cell monolayers in response to the proangiogenic chemokine IL-8 (24). We first observed that IL-8 stimulation induced a remarkable increase in endothelial monolayer permeability, comparable to that provoked by VEGF (Fig. 2A), as previously reported (34, 37). Chemical inhibition of VEGFR2 failed to block IL-8-induced permeability and ERK activation, while it prevented events downstream of VEGF (Fig. 2A). In contrast, the pharmacological inhibition of the chemokine receptor CXCR2 with SB^{225002} abolished IL-8-provoked ERK phosphorylation and the increase of endothelial permeability, without interfering with the effects of VEGF. SB^{225002} was identified as an antagonist of ^{125}I-labeled IL-8 binding to CXCR2 with a 50% inhibitory concentration of about 20 nM, displaying a 150-fold selectivity for CXCR2 over CXCR1 and multiple other G protein-coupled receptors (GPCRs) (51). The effectiveness of SB^{225002} as a CXCR2 inhibitor is further illustrated by the extinction of ERK phosphorylation in response to IL-8 in CXCR2-expressing HEK-293T cells (see Fig. S1 in the supplemental material). Furthermore, we engineered mouse endothelial cells deficient for CXCR2 by infections with lentivirus containing CXCR2 shRNA together with GFP (see Fig. S2 in the supplemental material). GFP-sorted cells expressing either a nonsilencing shRNA or two independent shRNA sequences for CXCR2 were then analyzed for CXCR2 protein expression. As shown in Fig. S2 in the supplemental material, CXCR2-deficient endothelial cells showed a markedly reduced activation of ERK upon IL-8 stimulation, which together with the effects of the chemical inhibitor SB^{225002}, provides evidence that IL-8 signals mainly through CXCR2 in mouse and human vascular endothelial cells.

Moreover, the stimulation of endothelial cells with ELR^+ chemokines, GROα (CXCL1), GROβ (CXCL2), and, to a lesser extent, GROγ (CXCL3), ENA-78 (CXCL5), and GCP-2 (CXCL6), which can act on the GPCR CXCR2 (1, 3), could also augment endothelial permeability (Fig. 2B). This increase in FITC-dextran passage could be hampered as well by the CXCR2 antagonist. In addition, IL-8 elicited PAK phosphorylation, as well as tyrosine and serine phosphorylation of the endothelium-specific adhesion molecule, VE-cadherin (Fig. 2C). All of these signaling events contribute to trigger cell-cell junction disorganization (19, 43, 48) (Fig. 1). However, short-term IL-8 exposure did not provoke full VEGFR2 activation (Fig. 2C), in contrast to that observed under prolonged stimulation with this chemokine under multilayered endothelial culture conditions (34). Thus, our data suggested that IL-8 and VEGF may both modify the endothelial barrier properties independently in an acute response.

Because the Rac/PAK signaling axis has emerged as a key regulatory mechanism controlling endothelial barrier development and function (18–20, 29, 43, 46), we investigated the contribution of this biochemical route to endothelial permeability downstream of IL-8 stimulation. First, we observed that, in addition to ERK, IL-8 exposure induces Rac activation in

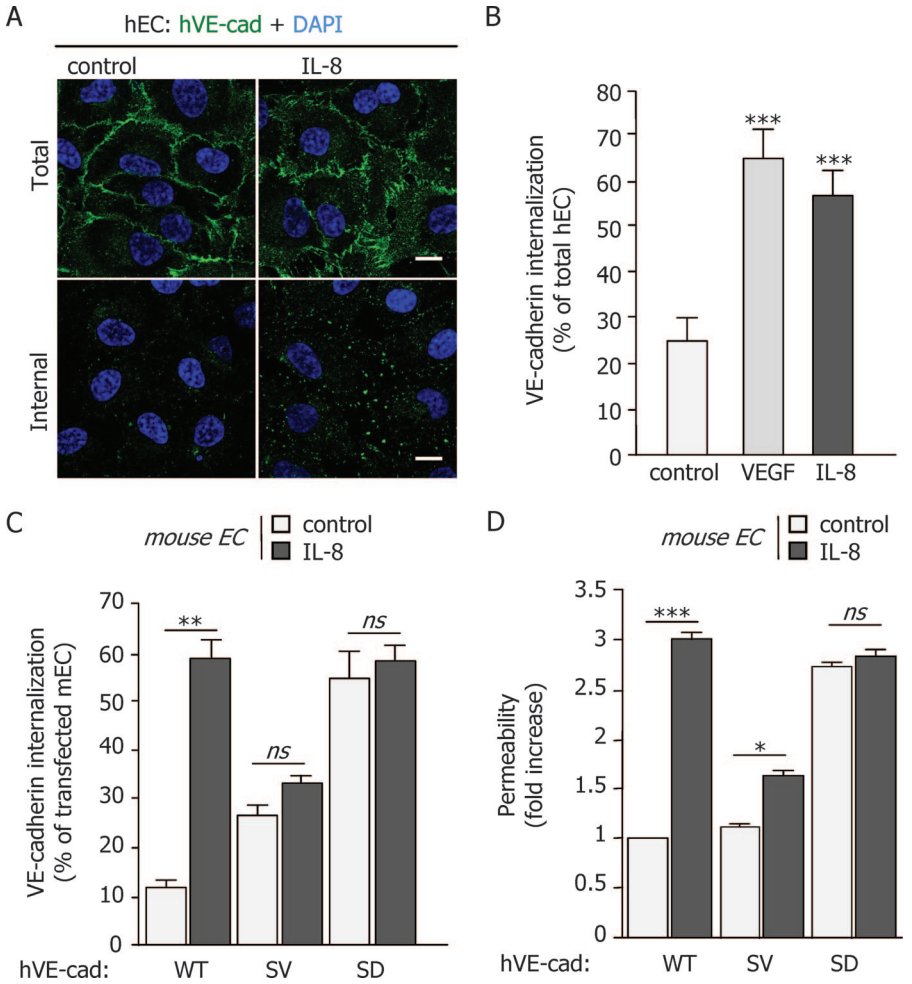

FIG. 1. VE-cadherin internalization is required for IL-8-induced endothelial monolayer permeability. (A) Three-day-old human endothelial cell (hEC) monolayers were starved overnight and were subjected to VE-cadherin (hVE-cad) staining (green) of living cells at 4°C and then left unstimulated (control) or exposed to IL-8 (50 ng/ml for 30 min) at 37°C. Either cells were fixed (total), or membrane-bound antibodies were stripped away by a mild acid wash before fixation (internal). Representative confocal acquisitions of VE-cadherin staining are shown. Counterstaining of nuclei with DAPI (4,6′-diamidino-2-phenylindole) is shown in blue. Scale bars, 10 μm. (B) Quantification of VE-cadherin uptake expressed as a percentage of internal VE-cadherin-positive cells to total cells under control conditions or VEGF- or IL-8-treated cells (50 ng/ml for 30 min) ($n > 300$). (C and D) Subconfluent mouse endothelial cells (mEC) were transfected with human VE-cadherin WT, its nonphosphorylatable S665V mutant (SV), and its phosphomimetic S665D mutant (SD) and then allowed to form a monolayer for 48 h before overnight starvation. Mouse endothelial cells were used in order to specifically track exogenous transfected human VE-cadherin in antibody uptake assays and similarly used in permeability assays. (C and D) VE-cadherin uptake quantification expressed as a percentage of internal VE-cadherin-positive cells to transfected mouse endothelial cells ($n > 300$ cells) (C) and permeability to FITC-dextran (D). ** and ***, $P < 0.01$ and $P < 0.001$, respectively, by ANOVA.

endothelial cells in a CXCR2-dependent manner (Fig. 2D). We then tested the involvement of Rac activation in endothelial permeability in response to IL-8 by reducing its expression by RNA interference, rather than by overexpression of mutant forms of Rac, as we noted that overexpression of both active and dominant-negative Rac mutants alters the endothelial barrier properties per se (see Fig. S3 in the supplemental material). Importantly, knocking down Rac resulted in a reduced activation of PAK, its direct downstream target, as well as a diminished phosphorylation of VE-cadherin on its S665 residue (Fig. 2E). This effect correlated with the inability of IL-8 to enhance the passage of fluorescein-conjugated dextran through endothelial monolayers, both when Rac expression was reduced and when the activity of PAK was blocked (Fig. 2F). Thus, PAK may act downstream from Rac to control the IL-8-dependent VE-cadherin phosphorylation and endothelial permeability.

PI3Kγ is involved in IL-8-induced increase of endothelial monolayer permeability. We then explored the nature of the IL-8/CXCR2-initiated pathway leading to the Rac- and PAK-dependent endothelial permeability. Surprisingly, whereas the blockade of Src kinases abolished the activation of Rac and the enhanced passage of fluorescein-conjugated dextran through endothelial monolayers in response to VEGF (Fig. 3A) (19), Src inhibition did not affect the stimulation of Rac and endothelial permeability when stimulated by IL-8 (Fig. 3A and B). This further suggests that the signaling pathway triggered by IL-8 diverges from the mechanism initiated by VEGF at the

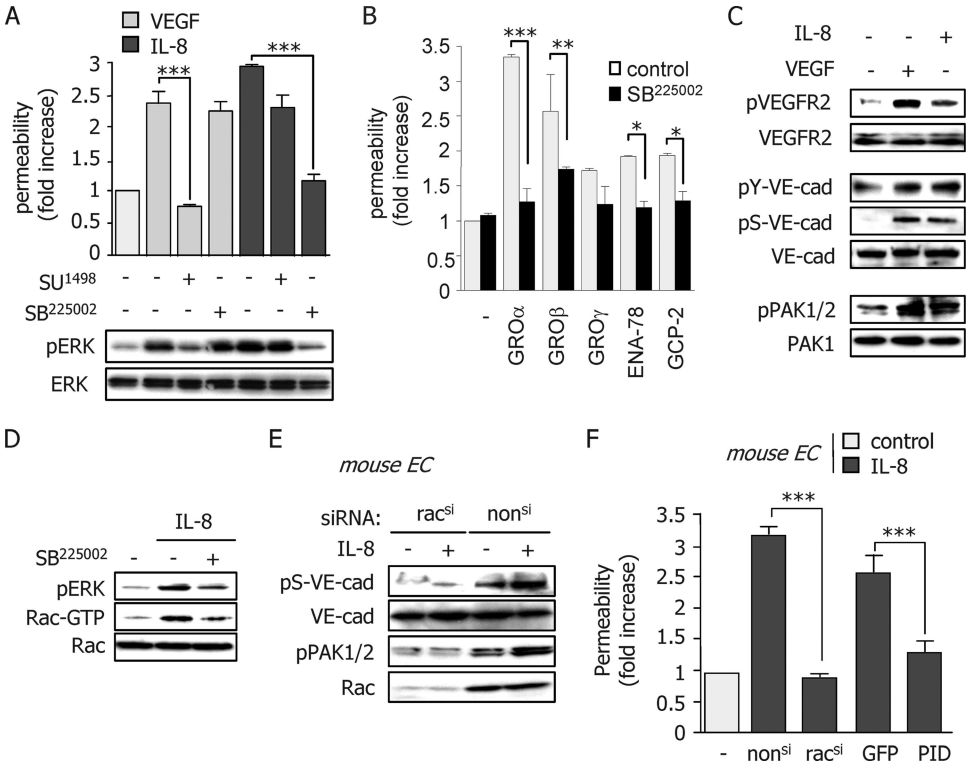

FIG. 2. IL-8 increases endothelial monolayer permeability through a CXCR2/Rac/PAK signaling axis. (A) Three-day-old human endothelial cell monolayers were starved overnight and incubated for 45 min with SU^{1498} (1 μM) or SB^{225002} (200 nM) and then stimulated either for permeability assays (upper panel; 30 min) or for total cell lysates (bottom panel; 5 min) with VEGF (50 ng/ml) and IL-8 (50 ng/ml). Untreated cells were used as a control (−). Permeability was expressed as increase with respect to untreated control cells. Total cell lysates were tested for phospho (p)-ERK1/2 and total ERK. (B) Three-day-old human endothelial cell monolayers were starved overnight and stimulated with GROα (CXCL-1), GROβ (CXCL-2), GROγ (CXCL-3), ENA-78 (CXCL-5), and GCP-2 (CXCL-6) (50 ng/ml for 30 min) in the presence of vehicle control (−) or SB^{225002} (200 nM 45 min pretreatment) before permeability assays were performed. (C) Using conditions similar to those described for panel A, Western blots were performed for pY1054-VEGFR2 (pVEGFR2), total VEGFR2, phosphotyrosine in VE-cadherin immunoprecipitates (pY-VE-cad), pS665-VE-cadherin (pS-VE-cad), total VE-cadherin (VE-cad), pT423-PAK1/pT402-PAK2 (pPAK1/2), and PAK1. (D) Cells were stimulated by IL-8 in the presence of vehicle (−) or SB^{225002} (200 nM 45 min pretreatment), and protein lysates were subjected to GST-CRIB pull-downs to affinity precipitate GTP-bound Rac. Total cell lysates were tested for pERK1/2 and total Rac. (E) Mouse endothelial cells (EC) were treated with RNA duplexes targeting mouse Rac (Rac^{si}) or nonsilencing sequences (non^{si}) (siRNA, 50 nM). Mouse endothelial cells were used in order to efficiently knock down mouse Rac1 by siRNA. Three days later, cell monolayers were starved overnight (−) and stimulated with IL-8 (+; 50 ng/ml for 5 min). Western blots were performed in total cell lysates for pS665-VE-cadherin, total VE-cadherin, pT423-PAK1/pT402-PAK2, and Rac. (F) Similarly treated cells were tested for FITC-dextran permeability. Alternatively, cells were electroporated with plasmids encoding GFP alone or fused to the PID and stimulated 3 days later with IL-8. ***, $P < 0.001$ by ANOVA.

level of Src, while both lead to endothelial permeability through Rac. In contrast, we observed a reduction of the VEGF- and IL-8-induced permeability by pretreating the cells with wortmannin, a general PI3K inhibitor (Fig. 3A). In addition, chemical inhibition of PI3K activity by LY^{294002} prevented IL-8-induced Rac and AKT activation in endothelial cells, as well as VE-cadherin phosphorylation, but left ERK activation intact (Fig. 3C).

As there are multiple isoforms of PI3K catalytic subunits which might play a distinct role downstream from GPCRs and tyrosine kinase receptors (5, 12, 50), we explored the ability to interfere selectively with the GPCR-initiated signaling route. To this aim, we knocked down various PI3K catalytic subunits using specific shRNA (Fig. 3D). The knockdown of the PI3Kγ catalytic subunit prevented the activation of Akt, a direct PI3K downstream target, as well as Rac activation and S665 VE-cadherin phosphorylation upon IL-8 stimulation (Fig. 3E). Interestingly, PI3Kγ knockdown did not alter acute ERK activation by IL-8, suggesting that a subset of CXCR2 signaling pathways are specifically affected by the absence of PI3Kγ (Fig. 3E). Importantly, we found that PI3Kγ knockdown strongly diminished the IL-8-induced endothelial permeability, while interfering with the expression of PI3Kα did not alter it (Fig. 3F). Therefore, blocking either CXCR2 or PI3Kγ selectively prevents the IL-8-provoked endothelial barrier disruption without affecting the VEGF-initiated response.

PI3Kγ has been recently shown as an integral signaling molecule involved in inflammation responses, which might in turn provoke vascular activation (4, 7, 24, 37, 42). Interestingly, a PI3Kγ-specific inhibitor, namely AS^{605240}, was used throughout these studies and has proven its efficiency in specifically blocking PI3Kγ activity in different cell targets (38). We therefore decided to assess whether AS^{605240} might also interfere with endothelial monolayer remodeling upon IL-8 exposure. First, we checked that AS^{605240} treatment did not modify CXCR2 expression at the plasma membrane (Fig. 4A). Impor-

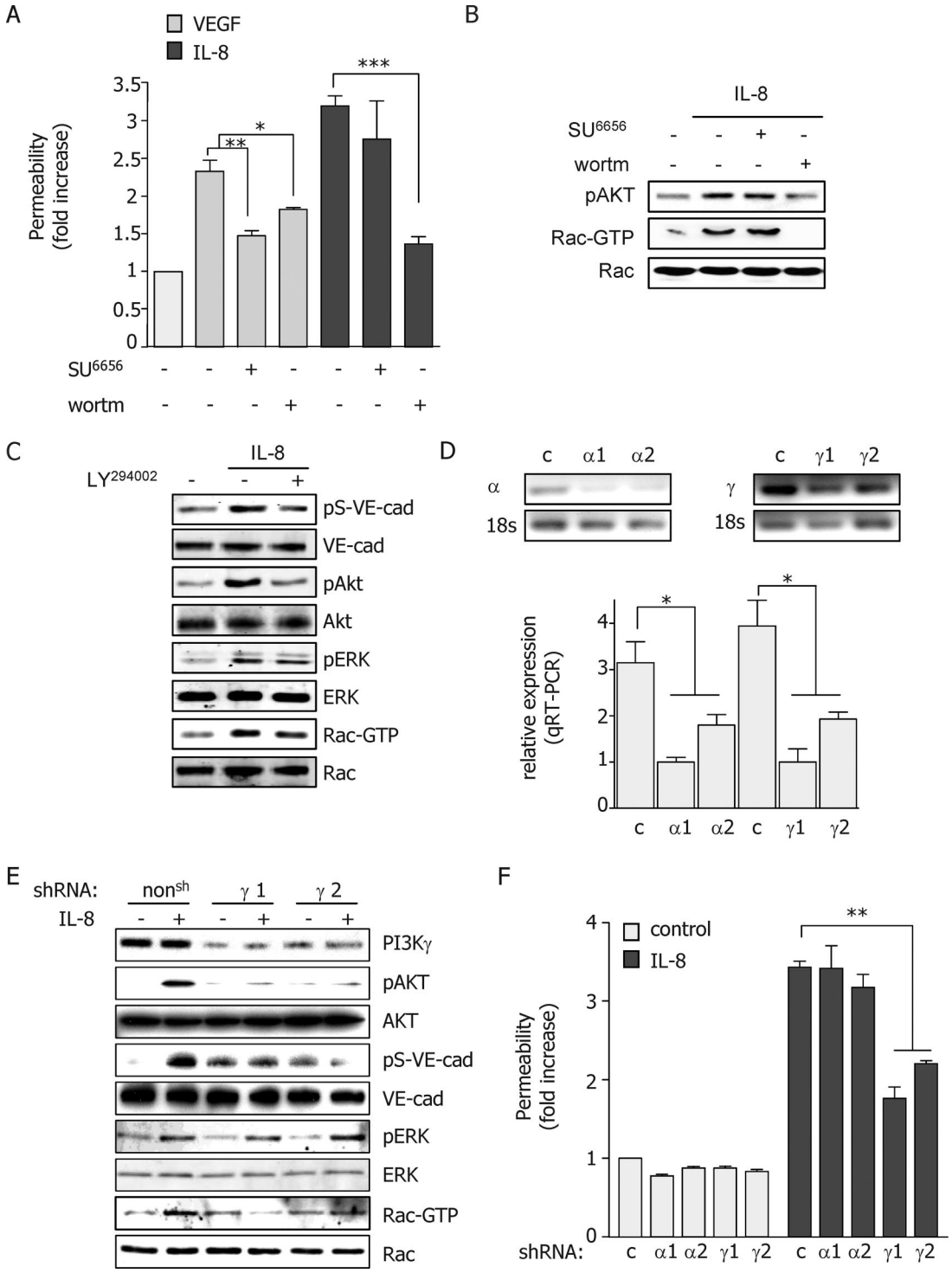

FIG. 3. PI3Kγ is involved in IL-8-induced increase of endothelial monolayer permeability. (A and B) Three-day-old human endothelial cell monolayers were starved overnight (−) and stimulated with IL-8 (50 ng/ml). Alternatively, cells were pretreated with the Src family kinase inhibitor SU^{6656} (1 μM for 45 min) or the general PI3K inhibitor wortmannin (wortm; 25 nM for 45 min). (A) Permeability assays in response to VEGF and IL-8 were performed as described previously, and (B) total cell lysates were blotted for pS473-Akt (pAkt) and Rac. GST-CRIB pull-down fractions were blotted against Rac (Rac-GTP). (C) Similarly, cells were treated with vehicle (−) and the PI3K inhibitor LY^{294002} (10 μM for 30 min) prior to IL-8 stimulation (+; 50 ng/ml for 5 min). Total cell lysates were analyzed for pS473-Akt, Akt, pERK1/2, ERK, pS665-VE-cadherin (pS-VE-cad), VE-cadherin (VE-cad), and Rac. Rac Western blots were also performed in GST-CRIB pull-down fractions (Rac-GTP). (D to F) Human endothelial cells were electroporated with mock (pLKO.1) or shRNA-containing plasmid directed against PI3K catalytic units α (α1 and α2) and γ (γ1 and γ2). (D) Five days later, total RNAs were extracted, quantified, and subjected to RT. Real-time PCR was performed on equal quantities of cDNA using oligonucleotides for PI3Kα and -γ and with 18S as a housekeeping gene. Aliquots of PCRs are shown, and the relative expression of PI3Kα and -γ in each shRNA-transfected cell population was assessed and is represented using arbitrary units. qRT-PCR, quantitative RT-CR. (E) Western blots for PI3Kγ, p-S473-Akt, total Akt, pS665-VE-cadherin, total VE-cadherin, and Rac were performed. GST-CRIB pull-down fractions were blotted against Rac (Rac-GTP). non^{sh}, non-shRNA transfected. (F) Permeability assays in response to IL-8 were performed 5 days later. *, **, and ***, $P < 0.05$, $P < 0.01$, and $P < 0.001$, respectively, by ANOVA.

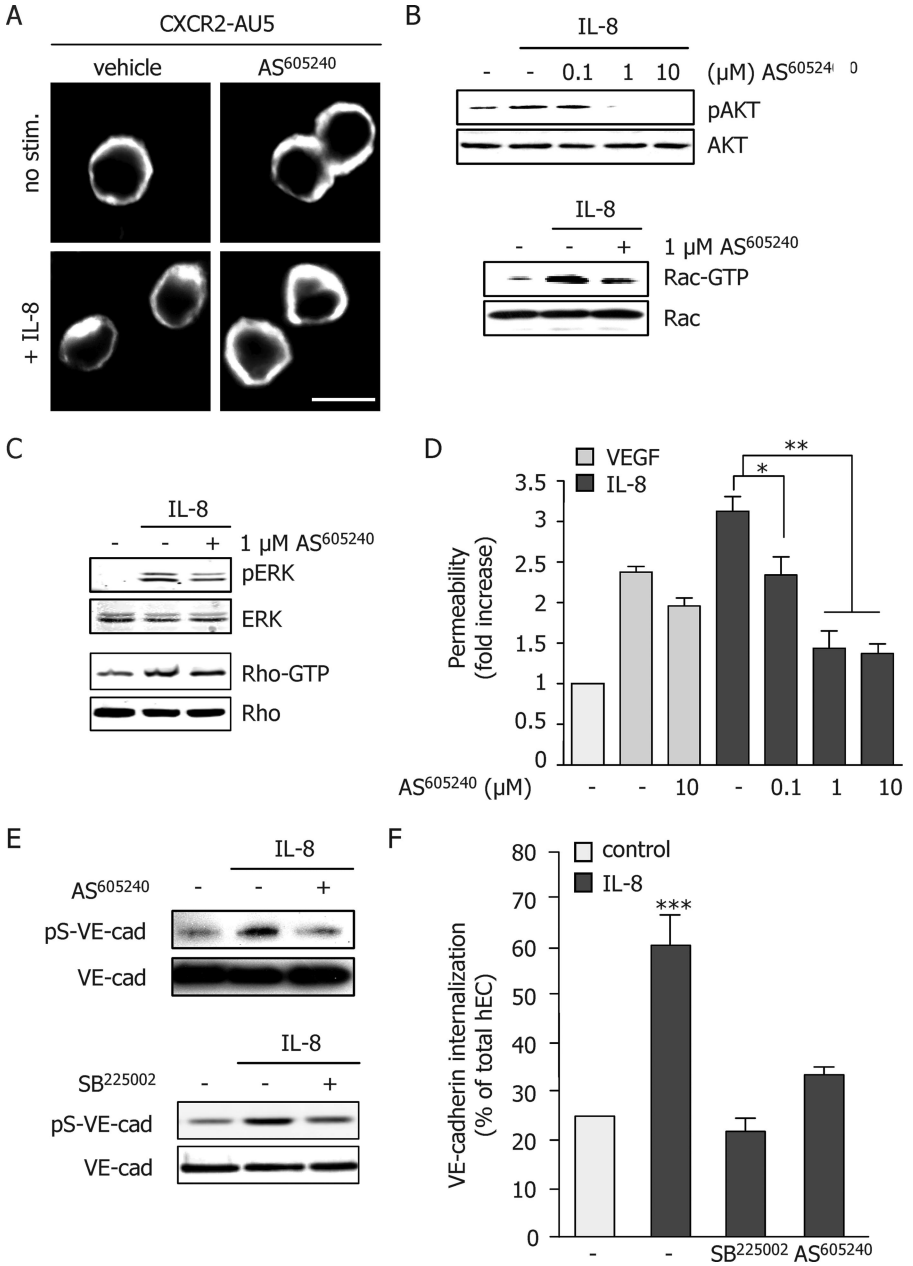

FIG. 4. PI3Kγ activity is required for the IL-8-dependent increase in endothelial monolayer permeability. (A) Human embryonic kidney cells (HEK-293T) were transfected with AU5-tagged CXCR2 DNA for 24 h prior overnight starvation. Cells were then treated with the PI3Kγ inhibitor AS^{605240} (1 μM for 45 min) and further stimulated with IL-8 (50 ng/ml for 30 min). Fixed samples were stained for AU5 and analyzed by confocal microscopy. Scale bar, 10 μm. no stim., no stimulation. (B and C) Three-day-old human endothelial cell monolayers were starved overnight (−), treated with the PI3Kγ inhibitor AS^{605240} (at the indicated concentrations or 1 μM for 45 min), and further stimulated with IL-8 (50 ng/ml for 5 min). Total cell lysates were blotted against p-S473-Akt (pAkt), total Akt, and total Rac in panel B and pERK1/2, ERK, and Rho in panel C. GST-CRIB (B) and GST-Rhotekin (C) pull-down fractions were blotted against Rac (Rac-GTP) and Rho (Rho-GTP), respectively. (D) Similarly AS^{605240}-treated cells were stimulated with VEGF or IL-8 (50 ng/ml for 30 min) and tested for permeability to FITC-dextran. (E and F) Three-day-old human endothelial cell monolayers were starved overnight (−), treated with SB^{225002} (200 nM for 45 min) or AS^{605240} (10 μM for 45 min), and then stimulated with IL-8 (50 ng/ml for 5 min). Western blots were performed in total cell lysates for pS665-VE-cadherin (pS-VE-cad) and total VE-cadherin (VE-cad). Shown are the results of quantification of VE-cadherin uptake expressed as a percentage of total cells, under control conditions, compared to that of IL-8-treated cells (50 ng/ml for 30 min), preincubated with vehicle (−), SB^{225002} (200 nM for 45 min), and AS^{605240} (10 μM for 45 min) ($n > 300$). *, **, and ***, $P < 0.05$, $P < 0.01$, and $P < 0.001$, respectively, by ANOVA.

tantly, the results we obtained by knocking down PI3Kγ in endothelial cells were recapitulated upon pharmacological treatment with AS^{605240}. Indeed, IL-8-dependent Rac activation and Akt phosphorylation were prevented by AS^{605240} pretreatment, while ERK and Rho activation were not (Fig. 4B and C). In addition, AS^{605240} interfered with IL-8, but not VEGF-triggered permeability (Fig. 4D). Finally, AS^{605240} also impeded the IL-8-induced serine phosphorylation of VE-cad-

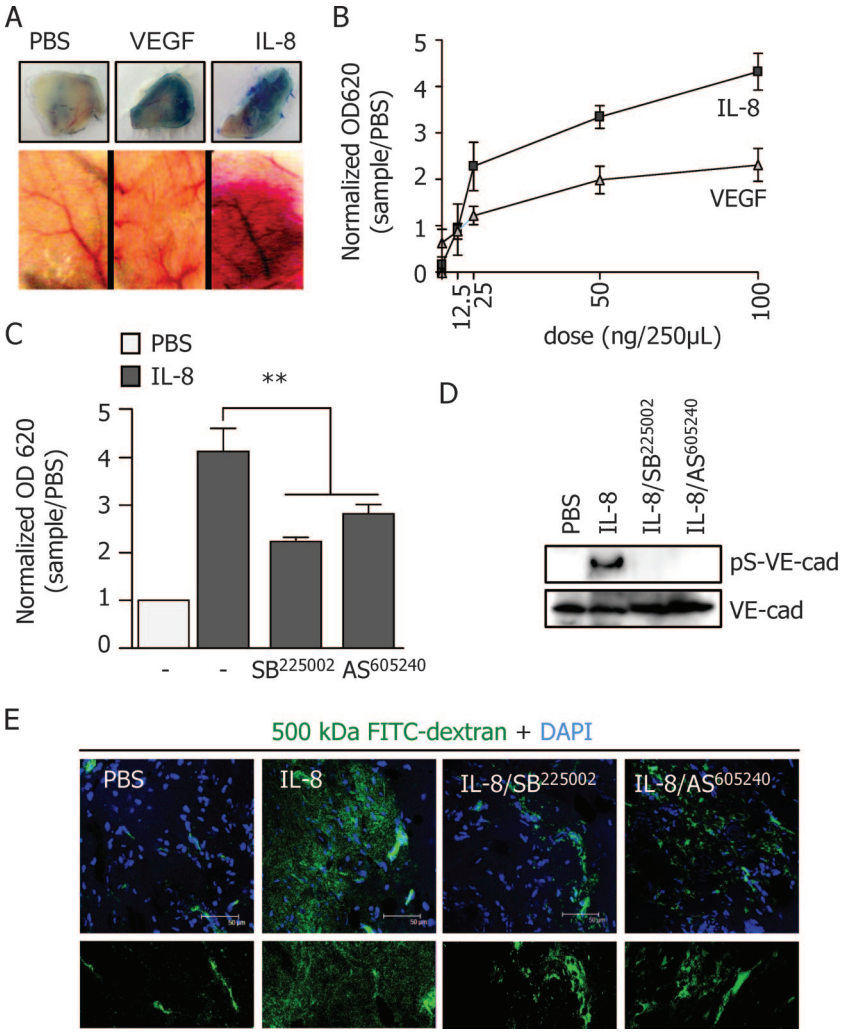

FIG. 5. Pharmacological inhibition of CXCR2 and PI3Kγ reduces IL-8-induced acute vascular permeability. (A and B) Mice were injected with PBS, VEGF (50 ng/250 μl), or IL-8 (50 ng/250 μl) subcutaneously shortly after EB injection in the tail vein. After 1 h, mice were sacrificed and injected skin samples were collected and photographed. Skin samples were then incubated in formamide for 36 h at 56°C, together with a noninjected similar skin area to serve as a background control. All samples were then filtered and read by spectrophotometry (optical density at 620 nm [OD 620]). The graph represents the ratio between the absorbance of control PBS-injected samples and that of skin of mice injected with the indicated concentrations of VEGF or IL-8. (C and D) Skin samples were treated as in panel B, with the following injections: PBS (250 μl) or IL-8 (50 ng/250 μl) alone or in combination with SB^{225002} (10 μM) and AS^{605240} (2 μM). Columns represent the ratio of the absorbance of skin from mice injected with IL-8 and CXCR2 and PI3Kγ inhibitors to that of the control-treated skins injected with PBS. Protein extracts were collected from fast-frozen similarly treated skin sections and analyzed by Western blotting for pS665VE-cadherin (pS-VE-cad) and total VE-cadherin (VE-cad). (E) Anesthetized rats were injected with FITC-conjugated 500-kDa dextran in the tail vein. The right ear was used as the PBS-injected control, while the left ear was injected with IL-8 alone (50 ng/10 μl) or with SB^{225002} (10 μM) or AS^{605240} (2 μM). After 1 h, animals were euthanized and their ears were cut, fixed in ethanol, and embedded for frozen sections. Representative pictures of FITC-conjugated 500-kDa dextran (green) and nucleus (blue; DAPI [4,6′-diamidino-2-phenylindole]) signals are shown. Scale bars, 50 μm. **, $P < 0.01$ by ANOVA.

herin and its endocytosis (Fig. 4E and F). Together, our data suggest that IL-8 utilizes a PI3Kγ/Rac/PAK pathway to promote VE-cadherin phosphorylation and endocytosis, thereby destabilizing the endothelial junctions.

Pharmacological inhibition of PI3Kγ reduces IL-8/CXCR2-induced acute vascular permeability. These findings prompted us to investigate the involvement of IL-8 in acute vascular permeability in vivo. For this effort, we first used a well-characterized mouse model of acute permeability based on the extravasation of EB after subcutaneous injections of permeability factors (20, 40, 49). As shown in Fig. 5A, IL-8 induced a robust extravasation of the EB in the surrounding tissue, accompanied by microhemorrhages, a phenotype that macroscopically appears more severe than those caused by VEGF. This effect was dose dependent, and IL-8-enhanced plasma leakage was nearly twofold greater than in response to VEGF after 1 h of exposure (Fig. 5B). Interestingly, while both VEGF and IL-8 converge on Rac to stimulate the PAK-dependent phosphorylation of VE-cadherin to increase endothelial permeability in vitro, IL-8 seems to be more potent than VEGF in vivo, as multiple cellular targets might be involved in the IL-8-induced vascular leakage.

Importantly, both CXCR2 and PI3Kγ blockers reduced the EB leakage caused by IL-8, as well as VE-cadherin S665 phosphorylation in dermal tissues (Fig. 5C and D). This effect was fast, as judged by time-lapse two-photon imaging of the extravasation of intravenously administered fluorescein-conjugated 500-kDa dextran, which is usually confined to the blood vessels (see Movie S1 in the supplemental material). Indeed, when IL-8 was applied locally in a small volume that does not allow diffusion, dextran-associated fluorescence was found massively in the surrounding tissue of the injection site in less than 10 min (Fig. 5E; see Movie S2 in the supplemental material). This leakage was significantly prevented when IL-8 was injected with the CXCR2 or PI3Kγ inhibitors (Fig. 5E). Together, our data demonstrate that IL-8 induces acutely vascular permeability in vivo, which can be impaired by blocking the CXCR2-initiated PI3Kγ signaling pathway.

Pharmacological inhibition of CXCR2 and PI3Kγ protects from laser-induced retinal damage. The proangiogenic and propermeability effects of IL-8 in acute and chronic situations and the fact that IL-8 has been shown to promote the development of leaky blood vessels and to elicit a proinflammatory phenotype in mouse retina (34, 37, 44, 53) prompted us to investigate the possibility of interfering with IL-8 function in a mouse model displaying laser-induced retinal damage. For these studies, we therefore utilized a well-established model of Bruch's membrane injuries (28, 39). In this case, a leaky blood vessel network is formed in choroidal neovascularized (CNV) areas, associated with the recruitment and the migration of inflammatory cells, such as macrophages and neutrophils, which in turn release proangiogenic and propermeability chemokines (17, 23, 53). First, we confirmed the increased production of VEGF-A in the CNV area 7 days after the laser-induced injuries, compared to that in normal mouse retina (Fig. 6A). Of interest, KC, the mouse homolog of IL-8, was also elevated in similar areas.

To test the possible involvement of IL-8 and its cognate receptor, CXCR2, in this pathological condition, mice were treated with intravitreal injections of the specific CXCR2 inhibitor SB^{225002} (36, 51) or with the solvent control, twice in each eye, on the day of the laser injuries and on day 3. After 7 days, the experiments were stopped and whole-mount choroids were stained with isolectin B4 in order to reveal neoformed blood vessels (Fig. 6B and C). The CXCR2 inhibitor dramatically limited the size of the neovascularized ocular lesions, to an extent comparable to that caused by the inhibition of VEGFR2 with SU^{1498} (Fig. 6B and C) (47). A higher concentration of the CXCR2 inhibitor allowed a more pronounced inhibition of the CNV, suggesting the efficacy of the targeting drug (data not shown). Of interest, the PI3Kγ inhibitor treatment, which was administered on the day of the injury and 3 days after, showed severe reduction of the lesion size after 7 days (Fig. 6B and C). Similar results were also observed later at 14 days, supporting a prolonged protective effect on CNV formation, without the need for repeated procedures (data not shown). Moreover, these laser-induced injuries showed an increase in the number of macrophages, infiltrated in the outer nuclear layer (ONL) and in the outer plexiform layer (OPL) (2, 23). Moreover, the reduction of retinal damage observed when SU^{1498}, SB^{225002}, and AS^{605240} were injected was concomitant with a decrease of infiltrated macrophages in the OPL, leaving intact the basal number of resident macrophages (Fig. 6D).

Tissue staining of the eye sections showed the morphology of the retina under normal conditions, where nuclear layers of neuronal cells exhibited a parallel alignment and normal retinal thickness (Fig. 6E). Laser injury on the Bruch's membrane induced the abnormal growth of choroidal blood vessels, as indicated by the formation of fibro-vascular structures between the choroid and the ONL (Fig. 6E). In the control vehicle-treated group, there were large CNV areas and obvious edema formation, as indicated by the greater retinal thickness and hump formation and the empty spaces between the choroid and the nuclear layers. Strikingly, this phenomenon was strongly reduced when animals received intravitreal injections of CXCR2 or PI3Kγ inhibitors, leaving only mild lesions, mainly caused by the direct physical wound provoked by the laser heat in the surrounding tissues (Fig. 6E). Similar results were obtained with the VEGFR2 inhibitor, as expected, reflecting the efficiency of anti-VEGF therapies (21). Thus, PI3Kγ and CXCR2 pharmacological inhibition can efficiently reduce retinal damage and hyperpermeability-associated ocular lesions, with similar benefits to blocking VEGFR activity.

DISCUSSION

Emerging findings indicate that IL-8 promotes endothelial permeability by initiating the activation of a CXCR2/PI3Kγ-regulated signaling pathway and that the pharmacological blockade of CXCR2 or PI3Kγ can efficiently reduce blood vessel leakage and laser-induced ocular lesions in vivo. This effect is likely dependent on the combined direct blockade of vascular permeability and proangiogenic effects of the mouse homolog of IL-8, KC, as well as on the ability to interfere with the acute macrophage activation and recruitment to the damaged retina, which may contribute together to neovascularization by providing growth and survival factors for the vascular bed (2, 5, 6, 23, 44, 53). Blocking CXCR2 and PI3Kγ activity in vivo could significantly reduce the laser-induced hyperpermeability in the retina, to an extent comparable to that achieved by blocking VEGFR2 activity. It will be important to assess in the future whether combination of therapies designed to target both IL-8 and VEGF might improve available treatment options for retinal hyperpermeability. Thus, the ability to inhibit the CXCR2/PI3Kγ signaling network and its multiple cellular targets may provide a novel strategy for pharmacological intervention in many human diseases that involve inflammation and enhanced vascular permeability, such as in neovascular age-related macular degeneration.

VEGF is the most described proangiogenic and propermeability factor, and interference with VEGF function has elicited considerable interest due to its clinical potential, in particular in the search for molecular approaches to interfere with tumor-induced angiogenesis and ocular diseases (16, 21, 31). However, despite clinical progress, recent reports have raised questions about potential adverse effects of anti-VEGF antibodies or its pharmacological inhibitors, as they may not only affect aberrant vessel outgrowth but also the normal vasculature (14, 15, 22) and may even induce permeability resembling VEGF stimulation in vivo (25). Other VEGF- and platelet-derived growth factor-related proangiogenic ligands have

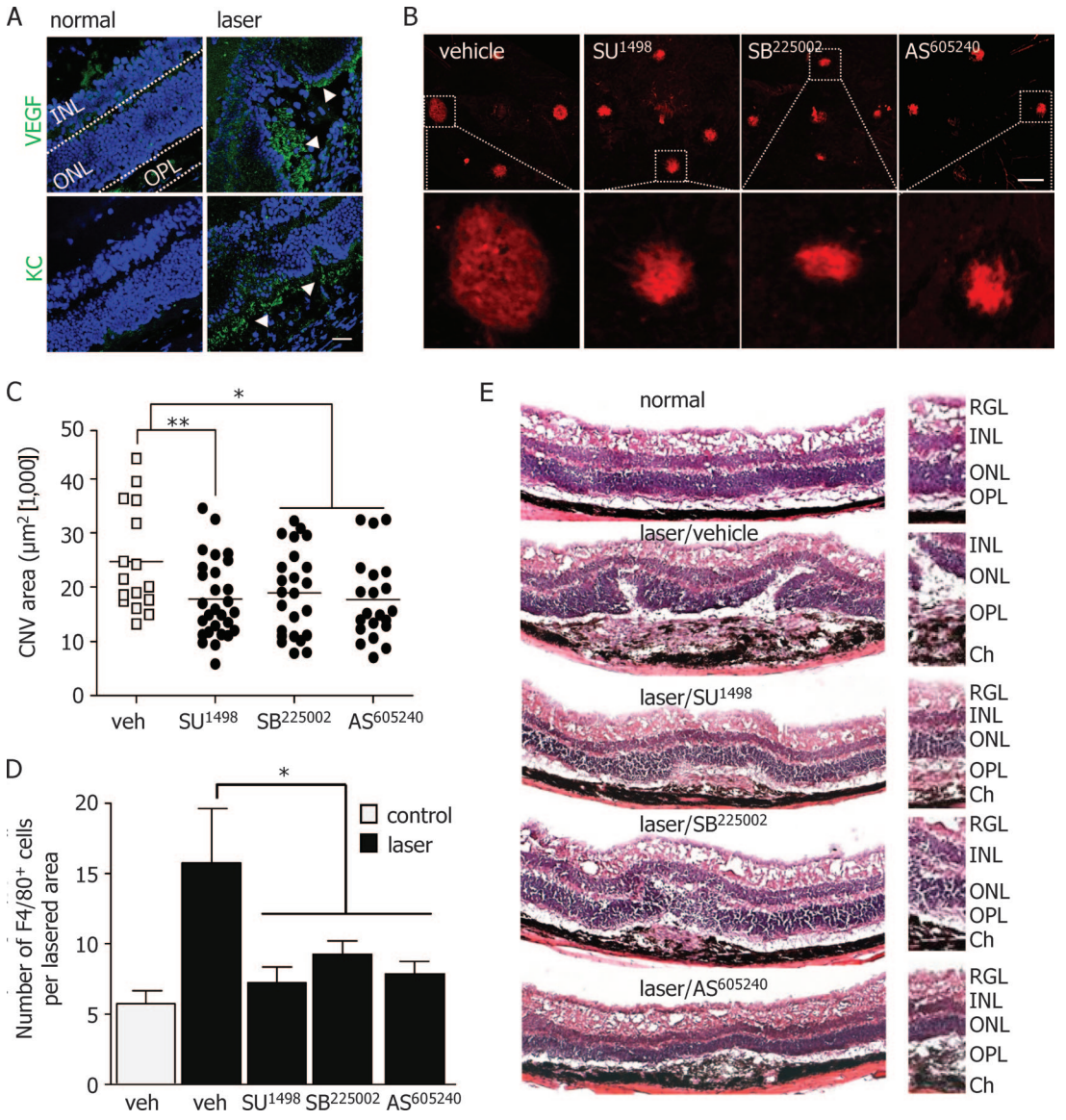

FIG. 6. Pharmacological inhibition of CXCR2 and PI3Kγ protects against laser-induced retinal damage. (A) Mice were injured by laser shots onto the retina as described in Materials and Methods (laser) or left untreated (normal), eyes were removed after 7 days, and frozen tissue sections were stained for VEGF-A and KC, the mouse homolog of IL-8 (green). Nuclei are shown in blue. (B to E) Laser-injured mice were injected intravitreally with vehicle (veh; 0.001% ethanol), VEGFR2 inhibitor SU^{1498} (10 μM), CXCR2 inhibitor SB^{225002} (10 μM), and AS^{605240} (50 μM) on days 1 and 3. Seven days later, mice were sacrificed and blood vessels were labeled with isolectin B4. (B) Representative pictures of each choroid with four neovascular areas, with higher magnification shown below. (C) Graphs represent the measure of the isolectin-positive area for each eyecup. (D) Frozen eye sections from similarly treated mice were stained for macrophages (F4/80 marker). The graph represents the number of positive F4/80 cells counted in the laser-injured area. Fields of similar sizes and locations were used in control retinas. (E) Eyes were extracted at day 7, cryosectioned, and stained with hematoxylin and eosin. RGL, retinal ganglion layer; INL, inner nuclear layer; Ch, choroid. Scale bars, 200 μm. * and **, $P < 0.05$ and $P < 0.01$, respectively, by ANOVA.

emerged as new targets in blocking blood vessel outgrowth (15, 27, 28, 41), as well as direct intracellular targets of the VEGF propermeability pathway, such as Src kinase (39). In this context, we observed that in laser-induced retinal vasculature lesions, IL-8 expression is increased concomitantly with VEGF expression in the damaged and inflamed retinal regions. Our data suggest that blocking CXCR2 might reduce vascular leakage and perivascular inflammation by preventing both endothelial permeability and acute recruitment of immune cells to the retinal wounds, thus halting the development of ocular lesions.

Of interest, whereas VEGF and IL-8 converge on Rac to stimulate the PAK-dependent phosphorylation of VE-cadherin to increase endothelial permeability, they both stimulate Rac activation by a divergent mechanism. Indeed, VEGF acts through the Src-family kinases to increase vascular leakage, while blocking Src activity in several mouse models for human diseases has successfully interfered with metastatic cell dissem-

ination, brain stroke neural damage, and neovascular ocular lesions (33, 39, 47). Interestingly, IL-8 does not require Src activity to stimulate Rac, but instead signals through a specific PI3K isoform, PI3Kγ, to promote Rac activation, thus resulting in endothelial cell-cell junction dismantlement. This observation provided an opportunity to selectively target the chemokine-initiated pathway by blocking PI3Kγ. Indeed, we obtained evidence that IL-8 induces a rapid and severe vascular leakage that can be efficiently prevented by the pharmacological inhibition of CXCR2 and PI3Kγ in vivo. Strikingly, CXCR2 and PI3Kγ inhibition dramatically limited the size of the ocular lesions, edema formation, and blood vessel growth, as well as the infiltration of macrophages at the site of injuries induced by laser burns.

Taken together, the ability to inhibit the CXCR2/PI3Kγ signaling network and its multiple cellular targets may provide a novel strategy to treat pathological neovascularization in damaged retina and in the tumor microenvironment, as many angiogenic mechanisms are similarly deregulated in ocular diseases and tumor vascularization (11). Furthermore, the ability to combine available FDA-approved drugs targeting VEGF-A with new therapeutic pharmacological inhibitors of IL-8 and its downstream signaling molecules may help identify additional treatment options for pathological neovascularization. Indeed, these studies may provide a rationale for the evaluation of anti-IL-8 and CXCR2 inhibitors or antibodies, as part of new multitargeted therapies in ocular diseases and other pathological conditions characterized by hyperpermeability of the vasculature.

ACKNOWLEDGMENTS

This research was supported by the Intramural Research Program of the NIH, National Institute of Dental and Craniofacial Research, and by funding from the Centre National de la Recherche Scientifique (CNRS), the Ligue Nationale contre le Cancer Region Ile-de-France, and the Projets Exploratoires/Premier Soutien (PEPS 2008) program held by CNRS.

We thank A. Sodhi (Wilmer Eye Institute, The Johns Hopkins Hospital, Baltimore, MD) for the initial cloning of CXCR2.

J.G., R.W., X.L., and J.S.G. planned the experimental design, J.G., X.H., Y.Q., D.M., and A.M. conducted the experiments, J.G., X.L., and J.S.G. analyzed data, and J.G. and J.S.G. wrote the paper.

We declare we have no competing financial interests.

REFERENCES

1. **Addison, C. L., T. O. Daniel, M. D. Burdick, H. Liu, J. E. Ehlert, Y. Y. Xue, L. Buechi, A. Walz, A. Richmond, and R. M. Strieter.** 2000. The CXC chemokine receptor 2, CXCR2, is the putative receptor for ELR+ CXC chemokine-induced angiogenic activity. J. Immunol. **165:**5269–5277.
2. **Ambati, J., A. Anand, S. Fernandez, E. Sakurai, B. C. Lynn, W. A. Kuziel, B. J. Rollins, and B. K. Ambati.** 2003. An animal model of age-related macular degeneration in senescent Ccl-2- or Ccr-2-deficient mice. Nat. Med. **9:**1390–1397.
3. **Balkwill, F.** 2004. Cancer and the chemokine network. Nat. Rev. Cancer **4:**540–550.
4. **Barber, D. F., A. Bartolome, C. Hernandez, J. M. Flores, C. Redondo, C. Fernandez-Arias, M. Camps, T. Ruckle, M. K. Schwarz, S. Rodriguez, A. C. Martinez, D. Balomenos, C. Rommel, and A. C. Carrera.** 2005. PI3Kgamma inhibition blocks glomerulonephritis and extends lifespan in a mouse model of systemic lupus. Nat. Med. **11:**933–935.
5. **Barberis, L., and E. Hirsch.** 2008. Targeting phosphoinositide 3-kinase gamma to fight inflammation and more. Thromb. Haemostasis **99:**279–285.
6. **Belperio, J. A., M. P. Keane, D. A. Arenberg, C. L. Addison, J. E. Ehlert, M. D. Burdick, and R. M. Strieter.** 2000. CXC chemokines in angiogenesis. J. Leukoc. Biol. **68:**1–8.
7. **Camps, M., T. Ruckle, H. Ji, V. Ardissone, F. Rintelen, J. Shaw, C. Ferrandi, C. Chabert, C. Gillieron, B. Francon, T. Martin, D. Gretener, D. Perrin, D. Leroy, P. A. Vitte, E. Hirsch, M. P. Wymann, R. Cirillo, M. K. Schwarz, and C. Rommel.** 2005. Blockade of PI3Kgamma suppresses joint inflammation and damage in mouse models of rheumatoid arthritis. Nat. Med. **11:**936–943.
8. **Carmeliet, P.** 2005. Angiogenesis in life, disease and medicine. Nature **438:**932–936.
9. **Dejana, E.** 2004. Endothelial cell-cell junctions: happy together. Nat. Rev. Mol. Cell Biol. **5:**261–270.
10. **Dirkx, A. E., M. G. Oude Egbrink, J. Wagstaff, and A. W. Griffioen.** 2006. Monocyte/macrophage infiltration in tumors: modulators of angiogenesis. J. Leukoc. Biol. **80:**1183–1196.
11. **Dorrell, M. I., E. Aguilar, L. Scheppke, F. H. Barnett, and M. Friedlander.** 2007. Combination angiostatic therapy completely inhibits ocular and tumor angiogenesis. Proc. Natl. Acad. Sci. USA **104:**967–972.
12. **Doukas, J., W. Wrasidlo, G. Noronha, E. Dneprovskaia, R. Fine, S. Weis, J. Hood, A. Demaria, R. Soll, and D. Cheresh.** 2006. Phosphoinositide 3-kinase gamma/delta inhibition limits infarct size after myocardial ischemia/reperfusion injury. Proc. Natl. Acad. Sci. USA **103:**19866–19871.
13. **Edgell, C. J., C. C. McDonald, and J. B. Graham.** 1983. Permanent cell line expressing human factor VIII-related antigen established by hybridization. Proc. Natl. Acad. Sci. USA **80:**3734–3737.
14. **Eremina, V., J. A. Jefferson, J. Kowalewska, H. Hochster, M. Haas, J. Weisstuch, C. Richardson, J. B. Kopp, M. G. Kabir, P. H. Backx, H. P. Gerber, N. Ferrara, L. Barisoni, C. E. Alpers, and S. E. Quaggin.** 2008. VEGF inhibition and renal thrombotic microangiopathy. N. Engl. J. Med. **358:**1129–1136.
15. **Fischer, C., B. Jonckx, M. Mazzone, S. Zacchigna, S. Loges, L. Pattarini, E. Chorianopoulos, L. Liesenborghs, M. Koch, M. De Mol, M. Autiero, S. Wyns, S. Plaisance, L. Moons, N. van Rooijen, M. Giacca, J. M. Stassen, M. Dewerchin, D. Collen, and P. Carmeliet.** 2007. Anti-PlGF inhibits growth of VEGF(R)-inhibitor-resistant tumors without affecting healthy vessels. Cell **131:**463–475.
16. **Folkman, J.** 2006. Angiogenesis. Annu. Rev. Med. **57:**1–18.
17. **Friedlander, M.** 2007. Fibrosis and diseases of the eye. J. Clin. Investig. **117:**576–586.
18. **Garrett, T. A., J. D. Van Buul, and K. Burridge.** 2007. VEGF-induced Rac1 activation in endothelial cells is regulated by the guanine nucleotide exchange factor Vav2. Exp. Cell Res. **313:**3285–3297.
19. **Gavard, J., and J. S. Gutkind.** 2006. VEGF controls endothelial-cell permeability by promoting the beta-arrestin-dependent endocytosis of VE-cadherin. Nat. Cell Biol. **8:**1223–1234.
20. **Gavard, J., V. Patel, and J. S. Gutkind.** 2008. Angiopoietin-1 prevents VEGF-induced endothelial permeability by sequestering Src through mDia. Dev. Cell **14:**25–36.
21. **Gragoudas, E. S., A. P. Adamis, E. T. Cunningham, Jr., M. Feinsod, and D. R. Guyer.** 2004. Pegaptanib for neovascular age-related macular degeneration. N. Engl. J. Med. **351:**2805–2816.
22. **Kamba, T., and D. M. McDonald.** 2007. Mechanisms of adverse effects of anti-VEGF therapy for cancer. Br. J. Cancer **96:**1788–1795.
23. **Kelly, J., A. Ali Khan, J. Yin, T. A. Ferguson, and R. S. Apte.** 2007. Senescence regulates macrophage activation and angiogenic fate at sites of tissue injury in mice. J. Clin. Investig. **117:**3421–3426.
24. **Koch, A. E., P. J. Polverini, S. L. Kunkel, L. A. Harlow, L. A. DiPietro, V. M. Elner, S. G. Elner, and R. M. Strieter.** 1992. Interleukin-8 as a macrophage-derived mediator of angiogenesis. Science **258:**1798–1801.
25. **Lee, S., T. T. Chen, C. L. Barber, M. C. Jordan, J. Murdock, S. Desai, N. Ferrara, A. Nagy, K. P. Roos, and M. L. Iruela-Arispe.** 2007. Autocrine VEGF signaling is required for vascular homeostasis. Cell **130:**691–703.
26. **Li, A., S. Dubey, M. L. Varney, B. J. Dave, and R. K. Singh.** 2003. IL-8 directly enhanced endothelial cell survival, proliferation, and matrix metalloproteinases production and regulated angiogenesis. J. Immunol. **170:**3369–3376.
27. **Li, X., M. Tjwa, L. Moons, P. Fons, A. Noel, A. Ny, J. M. Zhou, J. Lennartsson, H. Li, A. Luttun, A. Ponten, L. Devy, A. Bouche, H. Oh, A. Manderveld, S. Blacher, D. Communi, P. Savi, F. Bono, M. Dewerchin, J. M. Foidart, M. Autiero, J. M. Herbert, D. Collen, C. H. Heldin, U. Eriksson, and P. Carmeliet.** 2005. Revascularization of ischemic tissues by PDGF-CC via effects on endothelial cells and their progenitors. J. Clin. Investig. **115:**118–127.
28. **Li, Y., F. Zhang, N. Nagai, Z. Tang, S. Zhang, P. Scotney, J. Lennartsson, C. Zhu, Y. Qu, C. Fang, J. Hua, O. Matsuo, G. H. Fong, H. Ding, Y. Cao, K. G. Becker, A. Nash, C. H. Heldin, and X. Li.** 2008. VEGF-B inhibits apoptosis via VEGFR-1-mediated suppression of the expression of BH3-only protein genes in mice and rats. J. Clin. Investig. **118:**913–923.
29. **Liu, J., S. D. Fraser, P. W. Faloon, E. L. Rollins, J. Vom Berg, O. Starovic-Subota, A. L. Laliberte, J. N. Chen, F. C. Serluca, and S. J. Childs.** 2007. A βPix Pak2a signaling pathway regulates cerebral vascular stability in zebrafish. Proc. Natl. Acad. Sci. USA **104:**13990–13995.
30. **Marinissen, M. J., M. Chiariello, T. Tanos, O. Bernard, S. Narumiya, and J. S. Gutkind.** 2004. The small GTP-binding protein RhoA regulates c-jun by a ROCK-JNK signaling axis. Mol. Cell **14:**29–41.

30a. **National Research Council.** 1996. Guide for the care and use of laboratory animals. National Academy Press, Washington, DC.

31. **Olsson, A. K., A. Dimberg, J. Kreuger, and L. Claesson-Welsh.** 2006. VEGF

receptor signalling—in control of vascular function. Nat. Rev. Mol. Cell Biol. **7:**359–371.
32. **Orr, A. W., R. Stockton, M. B. Simmers, J. M. Sanders, I. J. Sarembock, B. R. Blackman, and M. A. Schwartz.** 2007. Matrix-specific p21-activated kinase activation regulates vascular permeability in atherogenesis. J. Cell Biol. **176:**719–727.
33. **Paul, R., Z. G. Zhang, B. P. Eliceiri, Q. Jiang, A. D. Boccia, R. L. Zhang, M. Chopp, and D. A. Cheresh.** 2001. Src deficiency or blockade of Src activity in mice provides cerebral protection following stroke. Nat. Med. **7:**222–227.
34. **Petreaca, M. L., M. Yao, Y. Liu, K. Defea, and M. Martins-Green.** 2007. Transactivation of vascular endothelial growth factor receptor-2 by interleukin-8 (IL-8/CXCL8) is required for IL-8/CXCL8-induced endothelial permeability. Mol. Biol. Cell **18:**5014–5023.
35. **Red-Horse, K., Y. Crawford, F. Shojaei, and N. Ferrara.** 2007. Endothelium-microenvironment interactions in the developing embryo and in the adult. Dev. Cell **12:**181–194.
36. **Reutershan, J.** 2006. CXCR2—the receptor to hit? Drug News Perspect. **19:**615–623.
37. **Reutershan, J., M. A. Morris, T. L. Burcin, D. F. Smith, D. Chang, M. S. Saprito, and K. Ley.** 2006. Critical role of endothelial CXCR2 in LPS-induced neutrophil migration into the lung. J. Clin. Investig. **116:**695–702.
38. **Ruckle, T., M. K. Schwarz, and C. Rommel.** 2006. PI3Kγ inhibition: towards an 'aspirin of the 21st century'? Nat. Rev. Drug Discov. **5:**903–918.
39. **Scheppke, L., E. Aguilar, R. F. Gariano, R. Jacobson, J. Hood, J. Doukas, J. Cao, G. Noronha, S. Yee, S. Weis, M. B. Martin, R. Soll, D. A. Cheresh, and M. Friedlander.** 2008. Retinal vascular permeability suppression by topical application of a novel VEGFR2/Src kinase inhibitor in mice and rabbits. J. Clin. Investig. **118:**2337–2346.
40. **Senger, D. R., S. J. Galli, A. M. Dvorak, C. A. Perruzzi, V. S. Harvey, and H. F. Dvorak.** 1983. Tumor cells secrete a vascular permeability factor that promotes accumulation of ascites fluid. Science **219:**983–985.
41. **Sennino, B., B. L. Falcon, D. McCauley, T. Le, T. McCauley, J. C. Kurz, A. Haskell, D. M. Epstein, and D. M. McDonald.** 2007. Sequential loss of tumor vessel pericytes and endothelial cells after inhibition of platelet-derived growth factor B by selective aptamer AX102. Cancer Res. **67:**7358–7367.
42. **Smith, D. F., T. L. Deem, A. C. Bruce, J. Reutershan, D. Wu, and K. Ley.** 2006. Leukocyte phosphoinositide-3 kinase γ is required for chemokine-induced, sustained adhesion under flow in vivo. J. Leukoc. Biol. **80:**1491–1499.
43. **Stockton, R. A., E. Schaefer, and M. A. Schwartz.** 2004. p21-activated kinase regulates endothelial permeability through modulation of contractility. J. Biol. Chem. **279:**46621–46630.
44. **Strieter, R. M., S. L. Kunkel, V. M. Elner, C. L. Martonyi, A. E. Koch, P. J. Polverini, and S. G. Elner.** 1992. Interleukin-8. A corneal factor that induces neovascularization. Am. J. Pathol. **141:**1279–1284.
45. **Taddei, A., C. Giampietro, A. Conti, F. Orsenigo, F. Breviario, V. Pirazzoli, M. Potente, C. Daly, S. Dimmeler, and E. Dejana.** 2008. Endothelial adherens junctions control tight junctions by VE-cadherin-mediated upregulation of claudin-5. Nat. Cell Biol. **10:**923–934.
46. **Tan, W., T. R. Palmby, J. Gavard, P. Amornphimoltham, Y. Zheng, and J. S. Gutkind.** 2008. An essential role for Rac1 in endothelial cell function and vascular development. FASEB J. **22:**1829–1838.
47. **Weis, S., J. Cui, L. Barnes, and D. Cheresh.** 2004. Endothelial barrier disruption by VEGF-mediated Src activity potentiates tumor cell extravasation and metastasis. J. Cell Biol. **167:**223–229.
48. **Weis, S., S. Shintani, A. Weber, R. Kirchmair, M. Wood, A. Cravens, H. McSharry, A. Iwakura, Y. S. Yoon, N. Himes, D. Burstein, J. Doukas, R. Soll, D. Losordo, and D. Cheresh.** 2004. Src blockade stabilizes a Flk/cadherin complex, reducing edema and tissue injury following myocardial infarction. J. Clin. Investig. **113:**885–894.
49. **Weis, S. M., and D. A. Cheresh.** 2005. Pathophysiological consequences of VEGF-induced vascular permeability. Nature **437:**497–504.
50. **Wetzker, R., and C. Rommel.** 2004. Phosphoinositide 3-kinases as targets for therapeutic intervention. Curr. Pharm. Des. **10:**1915–1922.
51. **White, J. R., J. M. Lee, P. R. Young, R. P. Hertzberg, A. J. Jurewicz, M. A. Chaikin, K. Widdowson, J. J. Foley, L. D. Martin, D. E. Griswold, and H. M. Sarau.** 1998. Identification of a potent, selective non-peptide CXCR2 antagonist that inhibits interleukin-8-induced neutrophil migration. J. Biol. Chem. **273:**10095–10098.
52. **Wong, T. Y., G. Liew, and P. Mitchell.** 2007. Clinical update: new treatments for age-related macular degeneration. Lancet **370:**204–206.
53. **Zhou, J., L. Pham, N. Zhang, S. He, M. A. Gamulescu, C. Spee, S. J. Ryan, and D. R. Hinton.** 2005. Neutrophils promote experimental choroidal neovascularization. Mol. Vis. **11:**414–424.